



Heat generation and radiation effects on steady MHD free convection flow of micropolar fluid past a moving surface

M. Gnaneswara Reddy*

Department of Mathematics, Acharya Nagarjuna University, Ongole Campus, Ongole 523 001, India

Article Info:

Received: 03/10/2011

Accepted: 17/10/2012

Online: 03/03/2013

Keywords:

Free convection,
MHD,
Radiation,
Heat generation.

Abstract

This paper was concerned with studying the magnetohydrodynamic steady laminar free convection flow of a micropolar fluid past a continuously moving surface in the presence of heat generation and thermal radiation. Similarity transformation was employed to transform the governing partial differential equations into ordinary ones, which were then solved numerically using the finite element method. Numerical results for the dimensionless velocity, microrotation and temperature profiles were obtained and displayed graphically for pertinent parameters to show interesting aspects of the solution. The skin friction and the rate of heat transfer were also computed and presented through tables. Favorable comparison with previously published work was performed.

Nomenclature

B_0	magnetic induction
C_f	skin-friction coefficient
c_p	specific heat at constant pressure
f	dimensionless stream function
G	microrotation parameter
G_1	microrotation constant
h	dimensionless microrotation
k	thermal conductivity
k_1	coupling constant
k_e	mean absorption coefficient
K	coupling constant
N	microrotation or angular velocity

Nu	Nusselt number
Pr	Prandtl number
q_r	radiative heat flux
Q	constant heat flux per unit area
R	radiation parameter
Re_δ	the Reynolds number
S	constant characteristic of the fluid
T	fluid temperature
T_w	surface temperature
T_∞	ambient temperature
u, v	velocity components in x - and y - directions, respectively
x, y	Cartesian coordinates along the sheet and normal to it, respectively

Greek Letters

α	thermal diffusivity
----------	---------------------

*Corresponding author
Email address: mgrmaths@gmail.com

β	thermal expansion coefficient
η	similarity variable
θ	dimensionless temperature
ϕ	heat generation parameter
κ	vortex viscosity
ν	kinematic viscosity
μ	dynamic viscosity
ρ	fluid density
σ	electrical conductivity of the fluid
σ_s	Stefan-Boltzmann constant
ψ	stream function

Subscripts

W	condition at the solid surface
∞	ambient condition

1. Introduction

A micropolar fluid is the fluid with internal structures in which coupling between the spin of each particle and the macroscopic velocity field is taken into account. It is a hydrodynamical framework suitable for granular systems which consists of particles with macroscopic size. The dynamics of micropolar fluids, originated from the theory of Eringen [1] has been a popular area of research. This theory may be applied to explain the flow of colloidal suspensions (Hadimoto and Tokioka [2]), liquid crystals (Lockwood et al. [3]), polymeric fluids, human and animal blood (Ariman et al. [4]) and many other situations. Ahmadi [5] presented solutions for the flow of a micropolar fluid past a semi-infinite plate while considering micro inertia effects. Soundalgekar and Takhar [6] studied the flow and heat transfer past a continuously moving plate in a micropolar fluid. Rees and Pop [7] studied free convection boundary layer flow of micropolar fluids from a vertical flat plate. The study of flow and heat transfer for an electrically conducting micropolar fluid past a porous plate under the influence of a magnetic field has attracted the interest of many investigators due to its applications in many engineering problems such as magneto hydrodynamic (MHD) generators, plasma studies, nuclear reactors, oil exploration, geothermal energy extractions and the boundary

layer control in the field of aerodynamics (Soundalgekar and Takhar [8]). A number of MHD studies have been carried out for examining the effects of magnetic field on hydrodynamic flow in various configurations like in channels and wedges, etc. (Takhar and Ram [9], Kumari [10]).

In many new engineering areas, processes (such as fossil fuel combustion energy processes, solar power technology, astrophysical flows and space vehicle re-entry) occur at high temperatures so knowledge of radiation heat transfer beside the convective heat transfer plays a very important role and cannot be neglected. Also, thermal radiation on flow and heat transfer processes is of major importance in the design of many advanced energy conversion systems operating at high temperature. Thermal radiation within these systems is usually the result of emission by hot walls and the working fluid. Thermal radiation effects become important when the difference between the surface and the ambient temperature is large. The Rosseland approximation is used to describe the radiative heat flux in the energy equation. On the other hand, heat transfer by simultaneous free convection and thermal radiation in the case of a polar fluid has not received much attention. This is unfortunate because thermal radiation plays an important role in determining the overall surface heat transfer in situations where convective heat transfer coefficients are small, as is the case with free convection, and such situations are common in space technology [11]. The flow and heat transfer from a continuous surface in a parallel free stream of micropolar fluid was studied by Gorla et al. [12]. The effect of radiation on heat transfer over a stretching surface was important in the context of space technology and the processes involving high temperature. Raptis [13] studied the flow of a micropolar fluid past a continuously moving plate by the presence of radiation. El-Arabawy [14] analyzed the problem of the effect of suction/injection on the flow of a micropolar fluid past a continuously moving plate in the presence of radiation. Seddeek et al. [15] investigated the analytical solution for the effect of radiation on flow of a

magneto-micropolar fluid past a continuously moving plate with suction and blowing magneto hydrodynamics; also, radiation effects on unsteady convection flow of micropolar fluid past a vertical porous plate with variable wall heat flux was studied by Gnanaswara Reddy [16].

The study of heat generation or absorption in moving fluids is important in the problems dealing with chemical reactions and those concerned with dissociating fluids. Possible heat generation effects may alter temperature distribution; hence, the particle deposition rate in nuclear reactors, electronic chips and semiconductor wafers. Recently, Gnanaswara Reddy [17] analyzed heat generation and thermal radiation effects over a stretching sheet in a micropolar fluid.

The main objective of the present study was to obtain the heat generation and thermal radiation effects of magneto hydrodynamic free convection flow of a micropolar fluid past a continuously moving surface. Using the similarity transformations, the governing equations were transformed into a set of ordinary differential equations, which were nonlinear and could not be solved analytically; therefore, finite element method was used for solving it. Numerical computations were performed for different values of the parameters to display the velocity, microrotation and temperature profiles graphically and to discuss the results from the physical point of view. The skin friction and rate of heat transfer were also computed for these parameters.

2. Mathematical formulation

The steady, two-dimensional flow of an incompressible electrically conducting micropolar fluid past a continuously moving sheet can be considered in the presence of heat generation and thermal radiation effects. The sheet was stretched with a linear velocity $u_w = Bx$, where B is a positive constant and x is the distance from the slit where the sheet originates. A uniform magnetic field of strength B_0 was assumed to be applied in the direction normal to the surface. The fluid

was assumed to be viscous and had constant properties. The applied magnetic field was assumed to be constant and the magnetic Reynolds number was assumed to be small so that the induced magnetic field was neglected. Under the usual boundary layer approximation, the governing equations were given as follows:

Continuity equation:

$$\frac{\partial u}{\partial x} + \frac{\partial v}{\partial y} = 0 \tag{1}$$

Momentum equation:

$$u \frac{\partial u}{\partial x} + v \frac{\partial u}{\partial y} = \nu \frac{\partial^2 u}{\partial y^2} + k_1 \frac{\partial N}{\partial y} + g\beta(T - T_\infty) - \frac{\sigma B_0^2}{\rho} u \tag{2}$$

Angular momentum equation:

$$G_1 \frac{\partial^2 N}{\partial y^2} - 2N - \frac{\partial u}{\partial y} = 0 \tag{3}$$

Energy equation:

$$u \frac{\partial T}{\partial x} + v \frac{\partial T}{\partial y} = \alpha \frac{\partial^2 T}{\partial y^2} - \frac{1}{\rho c_p} \frac{\partial q_r}{\partial y} + \frac{Q}{\rho c_p} (T - T_\infty) \tag{4}$$

The associated boundary conditions of Eqs. (1 – 4) can be written as:

$$u = Bx, \quad v = 0, \quad N = -\frac{1}{2} \frac{\partial u}{\partial y}, \quad T = T_w \quad \text{at } y = 0$$

$$u \rightarrow 0, \quad N \rightarrow 0, \quad T \rightarrow T_\infty \quad \text{as } y \rightarrow \infty \tag{5}$$

where u and v are the velocity components in the x and y direction, respectively, ρ is the density of the fluid, N is the microrotation component whose direction of rotation is in the xy plane, ν is the kinematic viscosity, G_1 is the microrotation constant, B_0 is magnetic induction, σ is electrical conductivity of the fluid, k is thermal conductivity, T is

temperature of the fluid in the boundary layer, T_∞ is the temperature of the fluid far away from the plate, α is thermal diffusivity, c_p is the specific heat at constant pressure, $k_1 = \frac{s}{\rho}$ is the coupling constant, s is a constant characteristic of the fluid and Q is constant heat flux per unit area.

By using the Rosseland approximation (Brewster [18]), the radiative heat flux q_r could be given by

$$q_r = -\frac{4\sigma_s}{3k_e} \frac{\partial T^4}{\partial y} \tag{6}$$

where σ_s is the Stefan-Boltzmann constant and k_e is the mean absorption coefficient.

It should be noted that, by using the Rosseland approximation, the present analysis was limited to optically thick fluids. If the temperature differences within the flow were sufficiently small, then, Eq. (6) could be linearized by expanding T^4 into the Taylor series about T_∞ , which might be in the following form after neglecting higher order terms

$$T^4 \cong 4T_\infty^3 T - 3T_\infty^4 \tag{7}$$

Considering Eqs. (6) and (7), Eq. (4) may be reduced to

$$u \frac{\partial T}{\partial x} + v \frac{\partial T}{\partial y} = \alpha \frac{\partial^2 T}{\partial y^2} + \frac{16\sigma_s}{3k_e \rho c_p} \frac{T_\infty^3}{\partial y^2} + \frac{Q}{\rho c_p} (T - T_\infty) \tag{8}$$

The velocity components u and v can be expressed in terms of the stream function ψ such that

$$u = \frac{\partial \psi}{\partial y} \text{ and } v = -\frac{\partial \psi}{\partial x}$$

It may be verified that the continuity equation was automatically satisfied. Also, the following non-dimensional variables can be introduced

$$\begin{aligned} \eta &= \left(\frac{B}{\nu}\right)^{1/2} y, \psi = (B\nu)^{1/2} x f(\eta), \theta = \frac{T - T_\infty}{T_w - T_\infty}, \\ N &= \left(\frac{B^3}{\nu}\right)^{1/2} x h(\eta), Gr = \frac{g\beta(T_w - T_\infty)}{xB^2}, \\ M &= \frac{\sigma B_0^2}{\rho B}, K = \frac{k_1}{\nu}, G = \frac{G_1}{\nu}, \\ Pr &= \frac{\nu \rho c_p}{k}, R = \frac{3k_e k}{16\sigma_s T_\infty^3}, \phi = \frac{2Q}{\rho c_p B} \end{aligned} \tag{9}$$

Considering Eq. (9), Eqs. (2), (3) and (8) can be transformed into the following ordinary nonlinear system of differential equations

$$f''' + ff'' - (f')^2 + Gr\theta - Mf' + Kg' = 0 \tag{10}$$

$$Gh'' - (2h + f'') = 0 \tag{11}$$

$$(1 + R)\theta'' + RPr f\theta' + RPr\phi\theta = 0 \tag{12}$$

The corresponding boundary conditions were

$$\begin{aligned} f = 0, f' = 1, h = -\frac{1}{2} f''(0), \theta = 1 \text{ at } \eta = 0 \\ f' \rightarrow 0, h \rightarrow 0, \theta \rightarrow 0 \text{ as } \eta \rightarrow \infty \end{aligned} \tag{13}$$

In the above equations, primes denote differentiation with respect to η where Gr is the thermal Grashof number, M is the magnetic field parameter, K is the coupling constant, G is microrotation parameter, R is radiation parameter, Pr is the Prandtl number and ϕ is the heat generation parameter.

For the type of flow under consideration, the physical quantities such as the wall shear stress and surface heat flux was very important, as could be given by

$$\tau_w = \mu \left(\frac{\partial u}{\partial y}\right)_{y=0} \tag{14}$$

$$q_w = -k \left(\frac{\partial T}{\partial y}\right)_{y=0} \tag{15}$$

where μ is viscosity and k is the thermal conductivity.

Hence, the skin-friction coefficient and Nusselt number near the plate in non-dimensional form can be given by

$$C_f = \frac{2\tau_w}{\rho u_w^2} = (\text{Re}_\delta)^{-1/2} f''(0) \quad (16)$$

$$Nu = \frac{xq_w}{k(T_w - T_\infty)} = -(\text{Re}_\delta)^{1/2} \theta'(0) \quad (17)$$

where $\text{Re}_\delta = \frac{u_w x}{\nu}$ is the Reynolds number.

3. Method of solution

The set of differential Eqs. (10 - 12) subjected to the boundary conditions (13) are highly nonlinear and coupled and therefore it cannot be solved analytically. Hence, following Reddy [19] and Bathe [20], the finite element method was used to obtain an accurate and efficient solution to the boundary value problem under consideration. The fundamental steps comprising the method were as follows:

Step 1: Discretization of the domain into elements:

The whole domain was divided to a finite number of *sub-domains*, a process known as discretization of the domain. Each sub-domain was termed a *finite element*. The collection of elements was designated the *finite element mesh*.

Step 2: Derivation of the element equations:

The derivation of finite element equations, i.e. algebraic equations, among the unknown parameters of the finite element approximation involved the following three steps:

- a. Constructing the variational formulation of the differential equation.
- b. Assuming the form of the approximate solution over a typical finite element.
- c. Deriving the finite element equations by substituting the approximate solution in variational formulation.

Step 3: Assembly of element equations:

The obtained algebraic equations were assembled by imposing the *inter-element*

continuity conditions, which yielded a large number of algebraic equations, constituting the *global finite element model*, which governed the whole flow domain.

Step 4: Impositions of boundary conditions:

The physical boundary conditions defined in Eq. (15) were imposed on the assembled equations.

Step 5: Solution of the assembled equations:

The final matrix equation could be solved by a direct or indirect (iterative) method. For computational purposes, the coordinate η varied from 0 to $\eta_{\max} = 6$, where η_{\max} represents infinity, i.e. external to the momentum, energy and concentration boundary layers. The whole domain was divided to a set of 100 line elements with equal width 0.05, each element being three noded. Thus, after assembling all the elements equations, a matrix of order 201×201 was obtained. This system of equations as obtained after assembly of the elements equations was non-linear; therefore, an iterative scheme was used for its solution. The system was linearized by incorporating known functions. After applying the given boundary conditions, only a system of 195 equations remained for the solution which was solved using Gauss elimination method. This process was repeated until the desired accuracy of 0.0005 was obtained (For detailed discussion of the method, see Gnaneswara Reddy and Bhaskar Reddy [21]).

4. Results and discussion

To verify the proper treatment of the problem, the numerical results were compared for Nusselt number $-\theta'(0)$ with those obtained by Raptis [13] for various values of M . The results of this comparison, given in Table 1, showed good agreement.

The distribution of the velocity, microrotation and temperature functions with the variation of Grashof number, material parameter, magnetic parameter, heat generation parameter and radiation parameter is shown graphically in Figs. 1-14. In the present study, the following

default parameter values of finite element computations were adopted:

$Gr = 1.0$, $K = 1.0$, $G = 1.0$, $M = 1.0$,
 $R = 1.0$, $\phi = 1.0$ and $Pr = 0.71$. All the graphs therefore corresponded to these values unless specifically indicated on the appropriate graph.

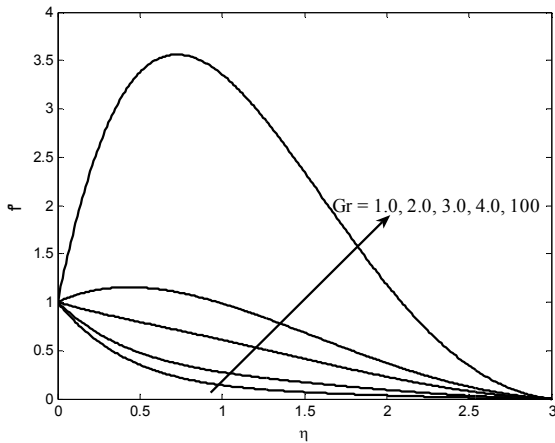


Fig. 1. Velocity distribution for different Gr .

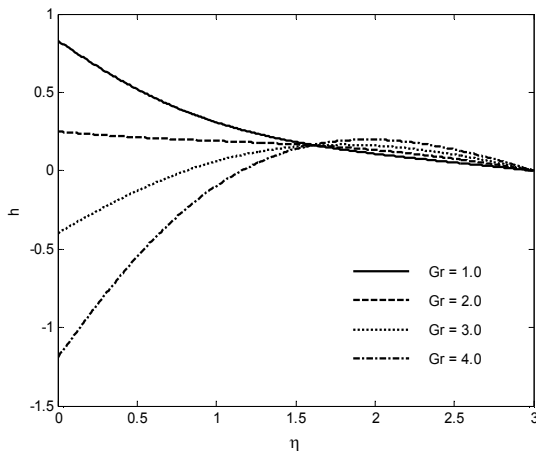


Fig. 2. Microrotation distribution for different Gr .

Figure 1 displays the results for the velocity distribution for various values of Gr . It is seen that velocity increases with the increase in Gr ; thereby, increasing the boundary layer. Figure 2 shows microrotation distribution with the variation of Gr . Microrotation decreased with the increase in Gr , which created a reverse rotation only near the boundary for large values of Gr . Figure 3 depicts the temperature distribution, which decreased with the increase

in Gr . It was observed that the cooling of fluid occurred within the boundary layer.

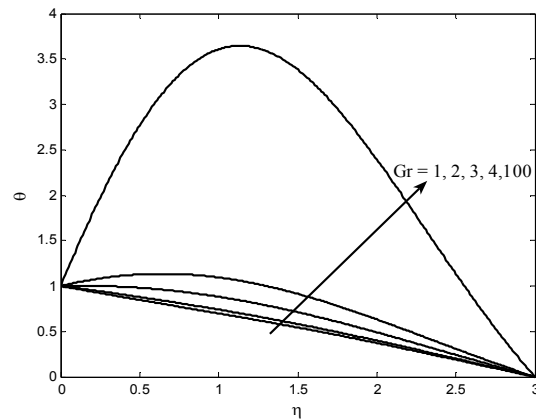


Fig. 3. Temperature distribution for different Gr .

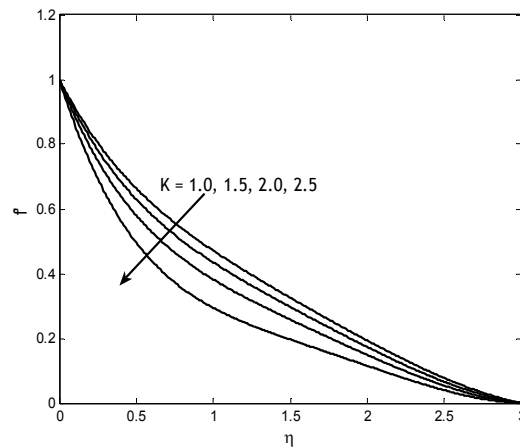


Fig. 4. Velocity distribution for different K .

Figure 4 shows the resulting dimensionless velocity profiles $f'(\eta)$ for various values of the material parameter K . It was observed that the velocity boundary layer thickness increased with increasing values of K associated with the decrease in the wall velocity gradient. Figure 5 shows the microrotation distribution with the variation of material parameter K . The microrotation increased with the increase in K . Figure 7 illustrates the velocity profile for different values of the magnetic parameter M . It showed that, for opposing flow, velocity decreased with the increase in M . It is demonstrated in Fig. 7 that the microrotation increased with the increase of M . Figure 8 represents the temperature distribution with the variation of magnetic parameter, which

increased with increase in magnetic parameter for the flow. Thus, the high temperature can be controlled by magnetic parameter M , which is required in many engineering applications.

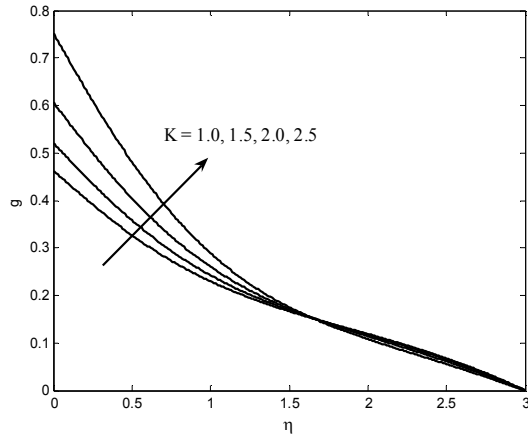


Fig. 5. Microrotation distribution for different K .

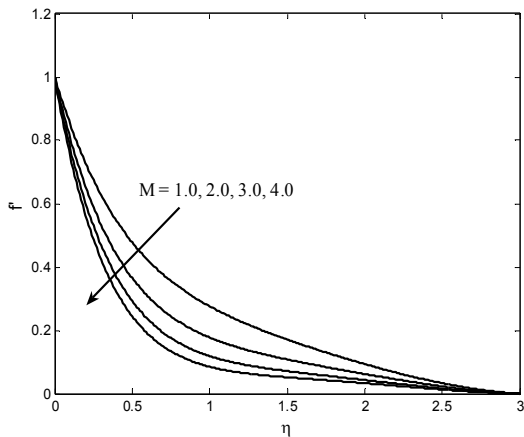


Fig. 6. Velocity distribution for different M .

Figures 9, 10 and 11 represent the effect of radiation parameter R on the velocity, microrotation and temperature functions, respectively. It is clear from the figures that the velocity and temperature decreased with the increase in R while microrotation increased with the increase in R .

Figure 12 shows the effect of heat generation parameter ϕ on f' . It could be observed that f' increased as the heat generation parameter ϕ increased. The effect of the heat generation parameter ϕ on g within the boundary layer region could be seen in Fig. 13. It is evident from this figure that g increased as

the heat generation parameter ($\phi > 0$) decreased.

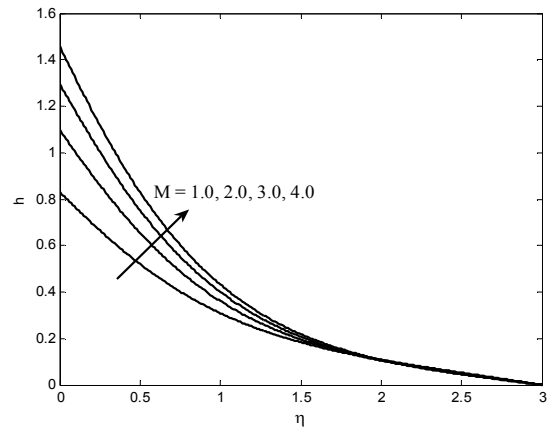


Fig. 7. Microrotation distribution for different M .

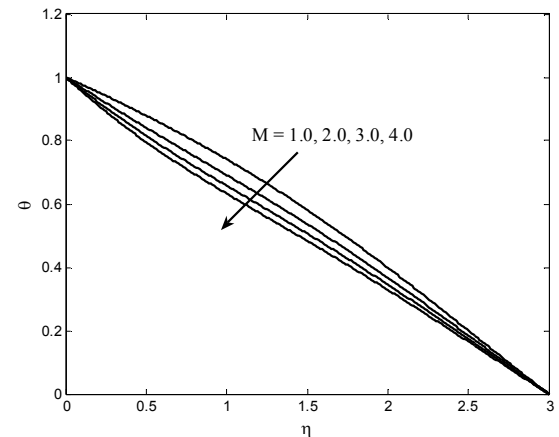


Fig. 8. Temperature distribution for different M .

Figure 14 displays effect of the heat generation parameter ϕ on θ . It can be observed that, as the heat generation parameter ϕ increased, the thermal boundary layer thickness increased. The skin-friction coefficient $f''(0)$ and the Nusselt number $-\theta'(0)$ for different values of Gr, K, M, R and ϕ are tabulated in Table 2. It is obvious from the table that the skin-friction coefficient numerically increased with the increase in M and K while decreasing with the increase in Gr, ϕ and R . The rate of heat transfer increased with the increase in Gr, ϕ and R while decreasing with the increase in K and M .

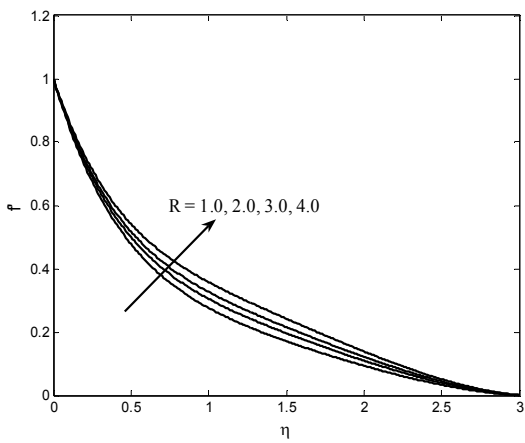


Fig. 9. Velocity distribution for different R .

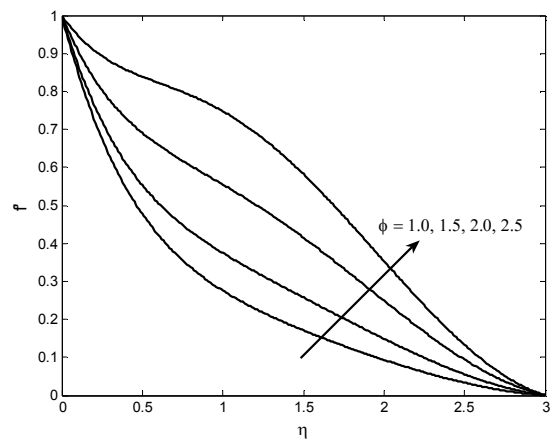


Fig. 12. Velocity distribution for different ϕ .

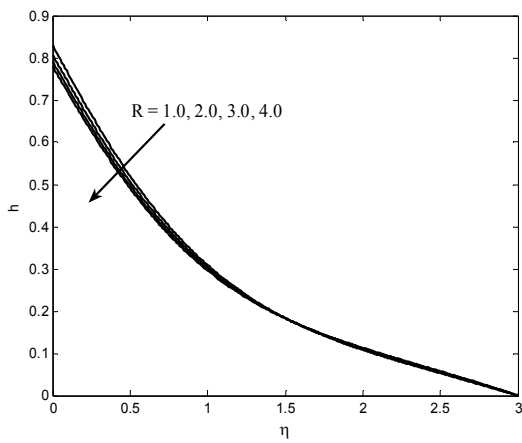


Fig. 10. Microrotation distribution for different R .

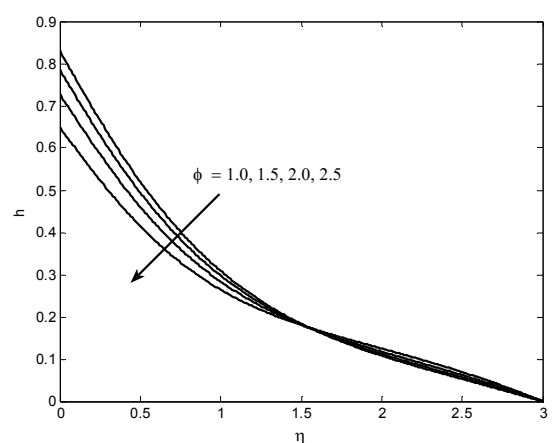


Fig. 13. Microrotation distribution for different ϕ .

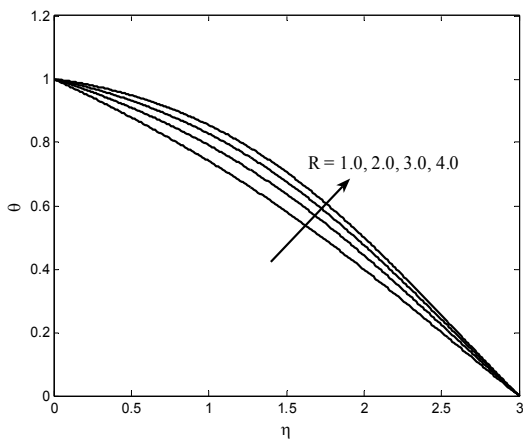


Fig. 11. Temperature distribution for different R .

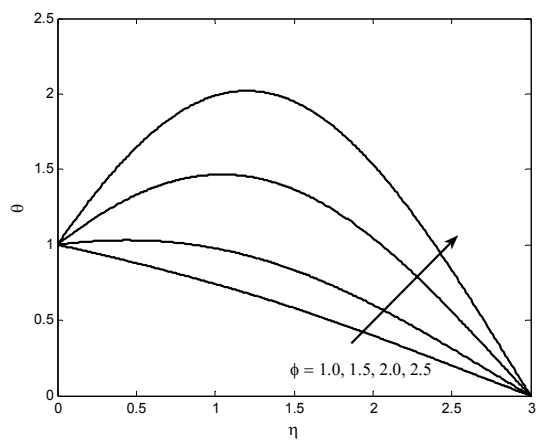


Fig. 14. Temperature distribution for different ϕ .

5. Conclusions

The steady two-dimensional laminar boundary layer MHD free convection flow of a micropolar fluid past a continuously moving surface was investigated. Different from previous investigations, the effect of thermal radiation and heat generation on the development of the thermal boundary layer flow was taken into consideration. The results were presented graphically and the conclusion was drawn that the flow field and other quantities of physical interest were significantly influenced by these parameters. Comparison with the previously published works was performed and excellent agreement was obtained between the results. The main conclusions of this study could be summarized as follows:

Table 1. Comparison of $-\theta'(0)$ for various values of M with $\phi = 0$.

M	Raptis [13]	Present Work
0	0.355590	0.355581
1	0.384224	0.384238
2	0.397385	0.397391
3	0.4044361	0.404432

Table 2. Numerical values of the skin-friction coefficient and the Nusselt number for $Pr = 0.71$.

Gr	K	M	ϕ	R	$f''(0)$	$-\theta'(0)$
1.0	1.0	1.0	1.0	1.0	0.925867	0.0647193
2.0	1.0	1.0	1.0	1.0	0.128817	0.126857
1.0	2.0	1.0	1.0	1.0	1.21334	0.0514129
1.0	1.0	2.0	1.0	1.0	1.42326	0.0430596
1.0	1.0	1.0	2.0	1.0	0.564008	1.11944
1.0	1.0	1.0	1.0	2.0	-0.66210	2.37658

The effects of a transverse magnetic field on an electrically conducting fluid caused a resistive-type force, called the Lorentz force. This force had the tendency to speed up the motion of the fluid. The result qualitatively agreed with the expectations since magnetic field exerted retarding force on the convection flow.

Application of a magnetic field moving with the free stream had the tendency to induce a motive force which decreased the motion of the fluid and increased its boundary layer.

The velocity and temperature decreased with the increase in R while microrotation increased with the increase in R .

The velocity and thermal boundary layer thicknesses increased by increasing the heat generation parameter whereas an opposite effect could be noted in the case of decreasing values of the heat generation parameter.

References

- [1] A. C. Eringen, "Theory of micropolar fluids", *J. Math. Mech.*, Vol. 16, pp. 1-18, (1966).
- [2] B. Hadimoto and T. Tokioka, "Two-dimensional shear flows of linear micropolar fluids", *Int. J. Eng. Sci.*, Vol. 7, pp. 515-522, (1969).
- [3] F. Lockwood, M. Benchaitra and S. Friberg, "Study of polytropic liquid crystals in viscometric flow and clasto hydrodynamic contact", *ASLE Tribology Trans.*, Vol. 30, pp. 539-548, (1987).
- [4] T. Ariman, M. A. Turk and N. D. Sylvester, "Microcontinuum fluid mechanics – a review", *Int. J. Eng. Sci.*, Vol. 12, pp. 273-293, (1974).
- [5] G. Ahmadi, "Self-similar solution of incompressible micropolar boundary layer flow over a semi- infinite plate", *Int. J. Eng. Sci.*, Vol. 14, pp. 639-646, (1976).
- [6] V. M. Soundalgekar and H. S. Takhar, "Flow of a micropolar fluid on a continuous moving plate", *Int. J. Eng. Sci.*, Vol. 21, p. 961, (1983).
- [7] D. A. S. Rees and I. Pop, "Free convection boundary layer flow of micropolar fluid from a vertical flat plate", *IMA J. Appl. Math.*, Vol. 61, pp. 179-197, (1998).
- [8] V. M. Soundalgekar and H. S. Takhar, "MHD forced and free convective flow past a semi-infinite plate", *AIAA J.*, Vol. 15, pp. 457-458, (1977).

- [9] H. S. Takhar and P. C. Ram, "Free convection in hydromagnetic flows of a viscous heat generating fluid with wall temperature and Hall currents", *Astrophys. Space Sci.*, Vol. 183, pp. 193-198, (1991).
- [10] M. Kumari, "MHD flow over a wedge with large blowing rates", *Int. J. Eng. Sci.*, Vol. 36, No. 3, pp. 299-314, (1998).
- [11] V. M. Soundalgekar, "Free convection effects on stokes problem for a vertical plate," *Journal of Heat Transfer*, Vol. 99, No. 3, pp. 499-501, (1977).
- [12] R. S. R. Gorla and P. V. Reddy, "Flow and Heat Transfer from a Continuous Surface in a Parallel Free Stream of Micropolar Fluid", *International Journal of Engineering Science*, Vol. 25, pp. 1243-1249, (1987).
- [13] A. Raptis, "Flow of a micropolar fluid past a continuously moving plate by the presence of radiation", *International Journal of Heat and Mass Transfer*, Vol. 41, No. 18, pp. 2865-2866, (1998).
- [14] H. A. M. El-Arabawy, "Effect of suction/injection on the flow of a micropolar fluid past a continuously moving plate in the presence of radiation", *International Journal of Heat and Mass Transfer*, Vol. 46, No. 8, pp. 1471-1477, (2003).
- [15] M. A. Seddeek, S. N. Odda, M. Y. Akl and M. S. Abdelmeguid, "Analytical solution for the effect of radiation on flow of a magneto - micropolar fluid past a continuously moving plate with suction and blowing", *Computational Materials Science*, Vol. 45, No. 2, pp. 423-42, (2009).
- [16] M. Gnaneswara Reddy, "Magnetohydrodynamics and radiation effects on unsteady convection flow of micropolar fluid past a vertical porous plate with variable wall heat flux", *ISRN Thermodynamics*, Vol. 2012, pp. 1-8, (2012).
- [17] M. Gnaneswara Reddy, "Heat generation and thermal radiation effects over a stretching sheet in a micropolar fluid", *ISRN Thermodynamics*, Vol. 2012, pp. 1-6, (2012).
- [18] M. Q. Brewster, *Thermal radiative transfer and properties*, John Wiley & Sons, New York, (1992).
- [19] J. N. Reddy, *An Introduction to the Finite Element Method*, McGraw-Hill, New York, (1985).
- [20] K. J. Bathe, *Finite Element Procedures*, Prentice-Hall, New Jersey, (1996).
- [21] M. Gnaneswara Reddy and N. Bhaskar Reddy, "Finite element analysis of solet and dufour effects on unsteady MHD free convection flow past an impulsively started vertical porous plate with viscous dissipation", *Journal of Naval Architecture and Marine Engineering*, Vol. 8, pp. 1-12, (2011).